Available online at www.sciencedirect.com

ScienceDirect

Procedia Structural Integrity 8 (2018) 83–91

Structural Integrity Procedia

www.elsevier.com/locate/procedia

AIAS 2017 International Conference on Stress Analysis, AIAS 2017, 6-9 September 2017, Pisa, Italy

Catadioptric stereo-vision system using a spherical mirror

S. Barone[a], P. Neri[a,*], A. Paoli[a] and A. V. Razionale[a]

[a]*University of Pisa, Department of Civil and Industrial Engineering, Largo L. Lazzarino 1, Pisa 56122, Italy*

Abstract

In the computer vision field, the reconstruction of target surfaces is usually achieved by using 3D optical scanners assembled integrating digital cameras and light emitters. However, these solutions are limited by the low field of view, which requires multiple acquisition from different views to reconstruct complex free-form geometries. The combination of mirrors and lenses (catadioptric systems) can be adopted to overcome this issue. In this work, a stereo catadioptric optical scanner has been developed by assembling two digital cameras, a spherical mirror and a multimedia white light projector. The adopted configuration defines a non-single viewpoint system, thus a non-central catadioptric camera model has been developed. An analytical solution to compute the projection of a scene point onto the image plane (forward projection) and vice-versa (backward projection) is presented. The proposed optical setup allows omnidirectional stereo vision thus allowing the reconstruction of target surfaces with a single acquisition. Preliminary results, obtained measuring a hollow specimen, demonstrated the effectiveness of the described approach.

Peer-review under responsibility of the Scientific Committee of AIAS 2017 International Conference on Stress Analysis

Keywords: 3D acquisition; structured light scanning; catadioptric stereo vision system; spherical mirror projection model; internal geometries acquisition

1. Introduction

The 3D reconstruction of mechanical parts is widely used in many branches of modern manufacturing industry to create digital models. In general, the shape of an existing physical model can be retrieved by using contact techniques

* Corresponding author. Tel.: +39-050-2218019; fax: +39-050-2218065.
E-mail address: paolo.neri@dici.unipi.it

Peer-review under responsibility of the Scientific Committee of AIAS 2017 International Conference on Stress Analysis
10.1016/j.prostr.2017.12.010

as in Hartig et al. (2012) , non-contact techniques as in Mian et al. (2015) or by exploiting multisensor approaches which integrate data deriving from different sensors as obtained by Barone et al. (2017) and Barone et al. (2017). Contact techniques make use of coordinate measuring machines or articulated arms, typically equipped with tactile probes, and provide accurate point-by-point measurements Hartig, Lin et al. (2012) . However, they only provide a limited number of measurements and are not suitable for the reconstruction of free-form shapes. On the other hand, non-contact techniques, as optical surface scanners (exploiting white light or laser light) or tomographic scanners, are able to perform full-field measurements. Among non-contact techniques, optical methods based on the triangulation principle provide full-field measurements with minimum user interaction Kevin (2013). Common arrangements are obtained by coupling a fringe projector with a single digital camera or two digital cameras assembled in a stereo rig. These solutions, however, are characterized by a limited field of view since projection and imaging devices must cover the same area. Catadioptric systems can be adopted to overcome this restriction. A catadioptric system is defined by the combination of single or multiple mirrors having different shapes (planar or curved) and lenses. The most used mirror shapes are those characterized by axial symmetry as spherical, parabolic, elliptical or hyperbolic, since they can cover the full azimuthal field of view. The viewed scene undergoes a transformation due to the reflection in the mirror. The projection of three-dimensional scene points to the corresponding two-dimensional points on the camera image plane can be obtained through a mapping function. The use of curved mirrors typically defines non-single viewpoint (non-SVP) sensors and introduces difficulties in the analytical modelling of the mapping function, which requires the calibration of the mirror geometry and pose with respect to the vision system Sturm et al. (2011). Stereo catadioptric configurations are required to provide the 3D reconstruction of a scene. Stereo vision is based on the common feature matching between two images taken from different positions. Depth is recovered by triangulating corresponding features on the images. Catadioptric omnidirectional stereovision can be obtained by using a single camera with at least two mirrors as in Fiala and Basu (2005) or in Jaramillo et al. (2016), two cameras and a single mirror as in Lin and Bajcsy (2003), two cameras and two mirrors as in Ragot et al. (2006) or in Boutteau et al. (2008). These configurations, however, define passive systems and are mainly used for robotic applications. When a 3D vision system is developed for metrological purposes, the passive stereo vision approach is not robust due to the difficulties in searching similar features in both images. For this reason, active approaches, based on the projection of structured patterns by a light emitter, are usually adopted. A catadioptric sensor based on a laser emitter, a camera and two hyperbolic mirrors is described in Orghidan et al. (2003). A similar approach is presented in Orghidan et al. (2006) where the pattern emitted by the laser diode is reflected by a conical mirror and a parabolic mirror is used to reflect the whole scene into the camera. A panoramic system composed of a white light projector, two parabolic mirrors and a digital camera is presented in Almaraz-Cabral et al. (2016). The system projects circular fringes and uses a temporal phase unwrapping technique to reconstruct the scene. However, this approach assumes that all the optical axes of the involved elements are coincident. Moreover, the projector must be calibrated in order to reduce the distortion influence.

In the present work, an active omnidirectional optical scanner has been developed by assembling two perspective digital cameras, a spherical mirror and a multimedia white light projector. The same mirror is used to reflect the structured patterns projected on the sphere by the light emitter and to reflect the 3D scene into the cameras, thus resulting in a more compact configuration. In the proposed approach, the projector is un-calibrated and not directly involved in the measurement process since the stereo triangulation is carried out by exploiting the two cameras. Spherical mirrors represent an attractive and practical solution to create catadioptric systems due to their low fabrication costs. The aim of the work is the definition of a non-contact system capable of 360-degree 3D reconstructions of internal cylindrical environments, which are typically characterized by accessibility restrictions. The adopted optical configuration defines a non-central catadioptric system. For this reason, a catadioptric camera model has been developed. An analytical solution to compute the projection of a scene point onto the image plane and vice-versa is presented. The calibration procedure follows a two-steps approach: firstly, a conventional calibration of the stereo rig (without the spherical mirror) is performed to determine intrinsic and extrinsic camera parameters. The mirror is then introduced in the system and an optimization process is carried out to determine the sphere radius and pose with respect to the cameras. Preliminary results obtained by acquiring a hollow cylinder with a conical housing demonstrated the effectiveness of the developed catadioptric stereo-vision setup.

2. Material and methods

2.1. Hardware set-up

The proposed catadioptric system is composed of a camera pair, a multimedia projector and a spherical mirror. The cameras are 8-bit monochrome CCD devices with a resolution of 1280 × 960 pixel (The Imaging Source DMK 41BU02), mounting 16 mm focal length lenses. The DLP projector is an OPTOMA EX330e, having resolution XGA 1024 × 768 pixels. The mirror is a convex spherical mirror with an Enhanced Aluminum coating (Edmund Optics, 50±0.1 mm). The optical setup is fixed by using an aluminum frame in order to obtain a stable positioning between the imaging sensors (baseline = 130 mm) and the mirror, which is joined to the frame, through a 3D-printed support, 300 mm far from the camera baseline (Fig. 1(a)). The adopted camera stereo setup requires the calibration of the relative positioning between the imaging devices and the mirror, while the projector is un-calibrated. For this reason, any variation in the projector placement does not affect the calibration parameters. Both imaging devices and multimedia projector are disposed in order to stare at the spherical mirror, which performs an enlargement of the field of view. The described optical scheme is also represented in Fig. 1(b).

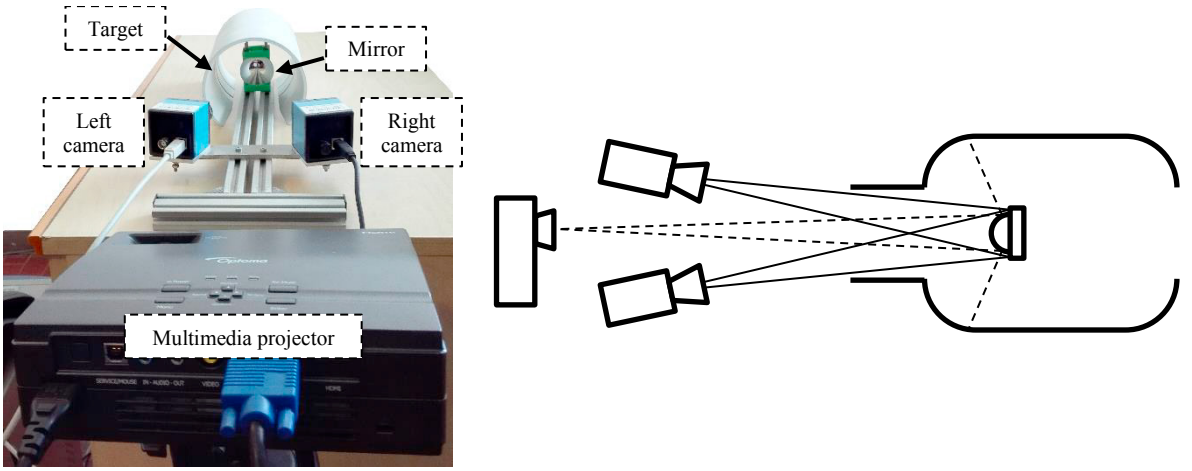

(a) (b)

Fig. 1. Catadioptric system setup: (a) cameras-mirror relative positioning and (b) full system during acquisition.

2.2. Non-central camera model

Spherical mirrors respect the SVP constraint when the camera pinhole is placed at the sphere's center Sturm, Ramalingam et al. (2011). This condition clearly does not represent an effective solution. A greater flexibility in the design of a catadioptric imaging system can be obtained by relaxing the SVP constraint. However, non-central catadioptric systems introduce difficulties in the analytical modelling of the mapping function and approximations are introduced if central models are used. The acquisition of an object projected onto a mirror can be schematized in two different problems: Forward Projection (FP), i.e. from the 3D point (X) to the 2D image location (x), and Backward Projection (BP), i.e. from the 2D pixel coordinates to the 3D direction passing from the corresponding 3D point on the scene. Some numerical solutions are available for both these problems in the case of spherical mirrors as described in Goncalves and Araujo (2009), but they result in time-consuming functions. Two different analytical closed form solutions were proposed by Agrawal et al. (2010) and Barone et al. (2017), exploiting different analytical formulations for the FP problem. In the present paper, the solution provided in Barone, Neri et al. (2017) has been used for both FP and BP problems. The BP problem can be easily solved by considering the scheme of Fig. 2(a): given the 2D coordinates of the point x on the image plane, the direction $\hat{p}$ can be obtained through the classical pinhole model, taking into account also terms for radial and tangential distortions (Sturm, Ramalingam et al. (2011)). Subsequently,

the intersection between the line passing by O (camera central point), with direction $\hat{p}$, and the sphere having centre c_s and radius r can be determined by solving a second degree polynomial function and selecting the solution closest to the origin, i.e the reflection point X_s. Finally, the direction $\hat{P}$ can be obtained by exploiting the reflection law (Yoshizawa (2015)). The FP problem solution is more complex, since neither the reflection point X_s nor the direction $\hat{p}$ are known. Thus, the problem is solved by looking for the intersection between the circle γ centred in c_s, and representing the section of the sphere with the solution plane, and the inner tangent ellipse Γ_i, having X and O as foci (Fig. 2(b)). It can be proven that this problem leads to a 4th degree polynomial form, which has four solutions: two solutions refer to the inner and outer ellipses Γ_i and Γ_o, and the other two solutions refer to the two tangent hyperbolae. The correct solution can be selected by choosing the one representing the ellipse having the smallest principal axes (i.e. Γ_o). Once the point X_s is determined, it is possible to find the 2D coordinates of the projected point x by using the pinhole model. The developed projection functions have been implemented in a matrix format in two different Matlab scripts ("*world2cam.m*" and "*cam2world.m*"), which are available for download at Matlab Central (Barone et al. (2017)). It is worth noting that the scripts also compute the Jacobian matrix of both FP and BP functions, which are extremely useful to speed up the optimization procedures carried out for the stereo-system calibration, as described in the following section.

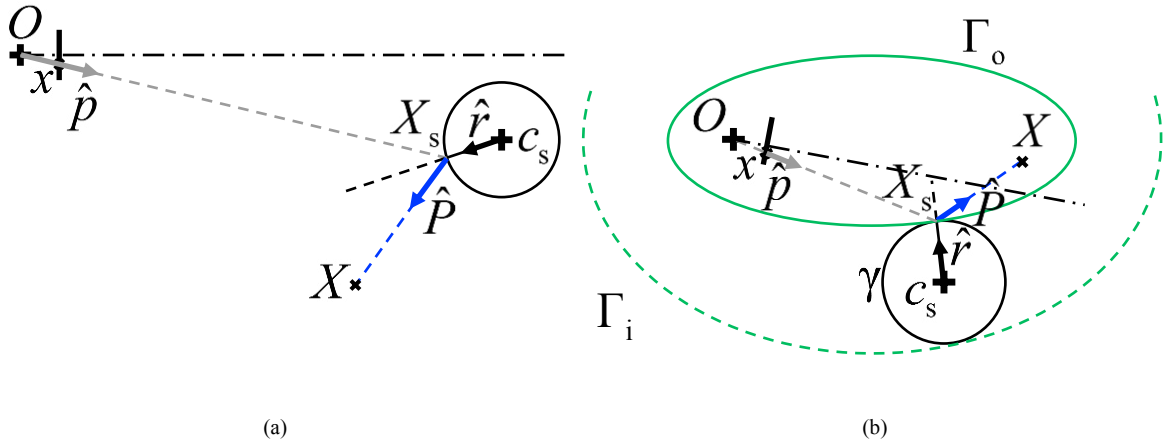

Fig. 2. Analytical model scheme: (a) Backward projection and (b) Forward projection.

2.3. Calibration process

The calibration process consists in the determination of the mirror geometry (i.e., radius value) and pose with respect to the vision system, and the determination of the relative placement between the two cameras. The adopted calibration procedure follows a two-steps approach: firstly, a conventional calibration of the stereo rig (without the spherical mirror) is performed to determine intrinsic and extrinsic parameters of the imaging devices Bouguet (2015). The mirror is then introduced in the system and fixed to the same rigid frame of the stereo-camera rig and an optimization process is carried out to determine sphere radius and pose with respect to the cameras, and to refine extrinsic parameters. Several different strategies are available to calibrate catadioptric systems based on curved mirrors: Scaramuzza et al. (2006), Puig et al. (2012) or Perdigoto and Araujo (2013). However, these approaches typically consider single camera systems with one or more mirrors. In the present work, the non-central projection model described in the previous section has been adopted to calibrate the assembled catadioptric stereo system. The procedure is based on the acquisition of a chessboard pattern (8×6 grid, 12 mm square size) imaged from different views by the stereo camera system. The reflection of the pattern on the spherical mirror, rather than the direct acquisition, was acquired by the camera pair. An example of the chessboard placement with respect to the camera pair

is shown in Fig. 3. The poses of the various acquired patterns were unknowns of the problem, and needed to be evaluated during the calibration process. For each acquisition, the 2D coordinates of the chessboard corners (reference coordinates) were automatically detected by using the approach proposed in Rufli et al. (2008). An optimization process was then carried out to determine the unknown parameters (i.e., mirror center and radius and chessboard poses). The 3D coordinates of each acquired chessboard (corresponding to the iterative tentative pose) was re-projected on the image plane by the FP function. The optimization target function was then defined as the differences between the re-projected coordinates and the reference ones. Each chessboard pose was defined by six scalar values: three values describing the 3D location of one of the grid points and three values describing the 3D orientation of the chessboard with respect to the reference frame (assumed to be the one centered on the left camera's central point and aligned with its optical axis). In this work, nine different chessboard placements have been used for the catadioptric system calibration, thus $6 \times 9 = 54$ optimization parameters were considered for the poses estimation. Moreover, three parameters were considered for the mirror center and one parameter was considered for the sphere radius. Finally, other six parameters were considered to define the roto-translation between right and left camera: the extrinsic parameters obtained in the first (conventional) calibration step were used as first guess and slightly refined in this second optimization step to achieve the final extrinsic parameters. Hence, an overall number of $54 + 4 + 6 = 64$ optimization parameters was considered in the optimization procedure. Table 1 reports the optimization procedure performances in terms of computational time (workstation, 18 GB of RAM and 64 bit operating system) and target function values.

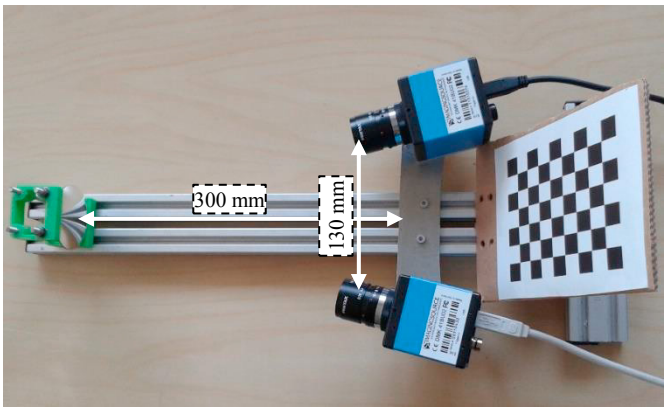

Fig. 3. Chessboard positioning during calibration process.

Table 1. Optimization process results.

	Left camera	Right camera
Time	46 s	
Final target function	16.1 pxl^2	
Max rep. dist.	0.3211 pxl	0.2797 pxl
Min rep. dist.	0.0083 pxl	0.0052 pxl
Mean rep. dist.	0.1385 pxl	0.1073 pxl
c_s	[-1.5 -8.7 291.9]^T mm	
R	50.1 mm	

The optimization procedure is fast and guarantees low re-projection errors, in the order of 0.1 pixels. Figure 4 shows a 2D plot of the re-projection errors in terms of x and y differences between the re-projected coordinates and the reference ones, for both left (Fig. 4(a)) and right camera (Fig. 4(b)). The plot shows a Gaussian distribution of the error, which is mainly due to the measurement uncertainty in the detection of the reference grid coordinates, thus confirming that the calibration procedure was successful. This hypothesis is also quantitatively validated by

performing a Royston's multivariate normality test Trujillo-Ortiz et al. (2007). Finally, Fig. 5 shows the results of the calibration procedure: Fig. 5(a) reports the overview of the calibrated system showing left and right camera central points, the spherical mirror and the calibration grids (the grid poses represent the results after the optimization process). Fig. 5(b) shows a single calibration grid with the optical rays corresponding to the first and last points of the grid.

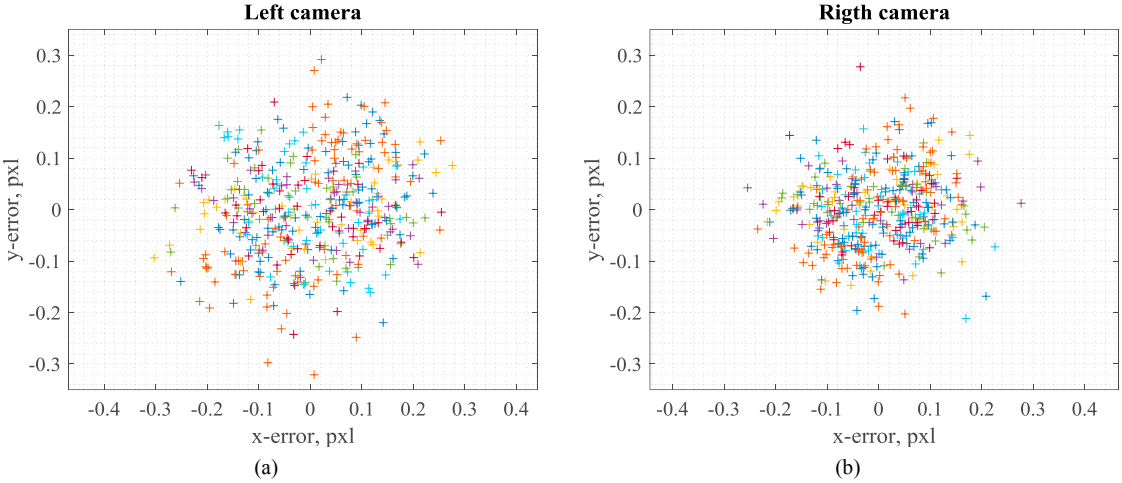

Fig. 4. Reprojection errors: (a) left camera and (b) right camera.

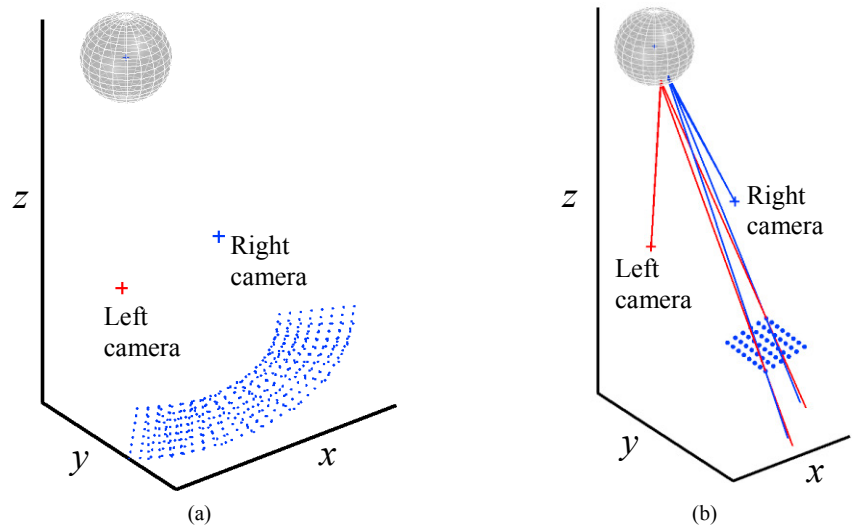

Fig. 5. Calibration procedure outcomes: (a) poses of the calibration grids and (b) stereo triangulation of two points.

2.4. Acquisition process

The calibration procedure described in the previous section uses the FP model for the optimization process. Once the catadioptric system is calibrated, 3D measurements are obtained by using the stereo triangulation principle. The stereo triangulation can be carried out if optical rays passing by the 3D points corresponding to the 2D points detected on left and right image planes are known. This result can be achieved by using the BP model. Thus, if a 3D point is viewed by both left and right cameras, it is possible to compute its placement on the scene by detecting the 2D

coordinates on both the image planes and intersecting the optical rays obtained by the BP function. In practice, these two lines do not intersect due to the measurement uncertainties. For this reason, the midpoint of the common perpendicular to the two rays corresponding to the matched points is used (Hartley and Sturm (1997)). The 3D reconstruction of a scene is then reduced to the detection of common features on left and right images (stereo-matching problem). Several different approaches, differentiating in passive and active methods, are available in literature. Passive methods are typically based on digital image correlation techniques carried out by exploiting speckle or texture patterns on the object surface. However, these approaches are not robust and result in low-density data, not suitable for full-field surface measurements. Active methods typically use fringe projection to encode the scene and solve the stereo-matching problem. In this paper, the DLP projector is used to project vertical and horizontal light stripes. A multi-temporal gray code phase shift profilometry (GCPSP) method is then used to encode and reconstruct the scene as described in Barone, Paoli et al. (2017). Fringe projection for internal geometries is a challenging task, which can be solved by using the spherical mirror: the fringe patterns are projected on the mirror, which reflects them on the target surface. The striped patterns on the target are then reflected back to the cameras by the mirror surface.

3. Results

The proposed catadioptric stereo system has been used to acquire the internal geometry of a target object characterized by a hollow cylinder with a conical housing. The mirror has been placed within the cylindrical region close to the intersection with the cone. Also, a planar surface has been placed close to the mirror on the bottom region. The 360° capabilities of the presented system (both of the camera and of the projector, since all the optical equipment field of view was expanded by the spherical mirror) allowed to reconstruct the entire geometry with a single acquisition. Fig. 6 shows a close view of the scene during the acquisition process.

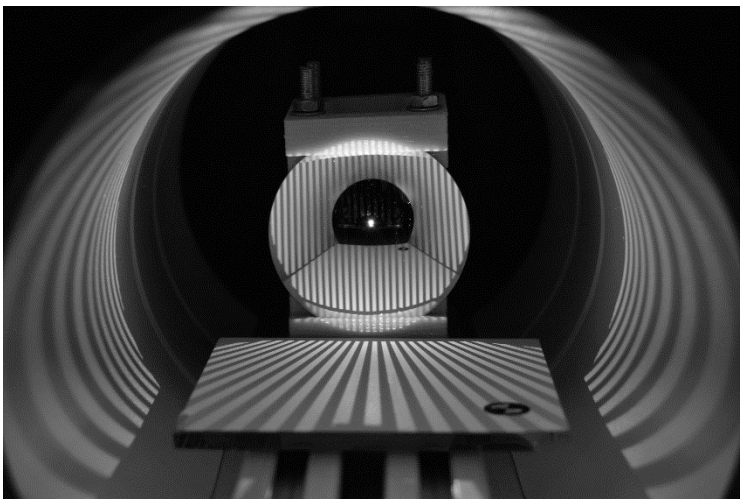

Fig. 6. Close view of the 360° acquisition: concave specimen and plane along with the projected pattern.

The internal geometry of the specimen and the planar surface are visible, lighted by the structured light pattern reflected by the mirror. The spherical mirror, imaged in the central part of the picture, shows the reflected geometries to be acquired. Fig. 7(a) reports the point cloud obtained for a single acquisition. Planar, cylindrical and conical primitive surfaces have been used to best fit the point cloud (Fig. 7(b-c)). Table 2 reports the results of the comparison carried out between acquired data and nominal dimensions. A really good agreement between nominal and measured dimensions can be observed along with an acceptable standard deviation for all the acquired geometries. It is worth noting that the lower standard deviation has been found for the planar surface, which is the geometry closest to the mirror. On the other hand, an increase of the noise level can be noted for higher distances of the measured surfaces, which is the case of the cylindrical and, more significantly, of the conical surfaces (Fig. 7(c)).

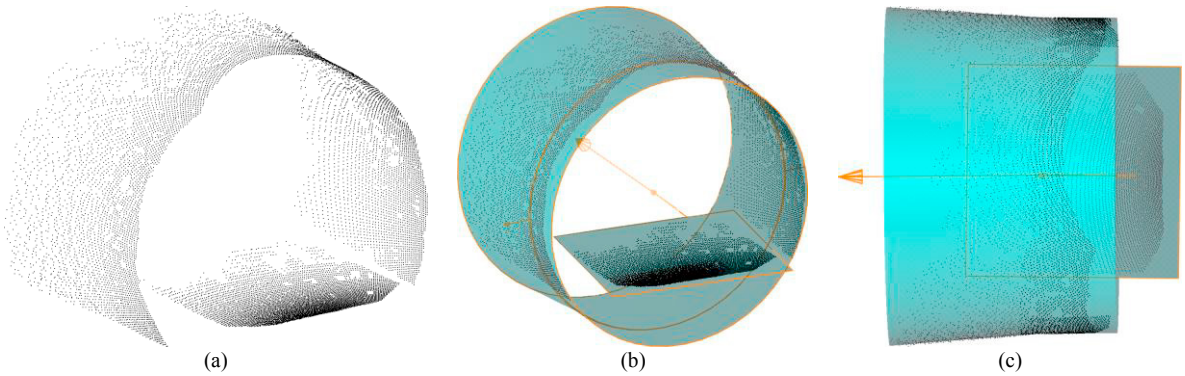

(a) (b) (c)

Fig. 7. Measured point cloud and best fit primitives.

Table 2. Measurement results.

	Measured	Nominal
Cone angle	4.3°	4°
Cylinder diameter	115.82 mm	115 mm
Cone std. deviation	0.33 mm	
Cylinder std. deviation	0.16 mm	
Plane std. deviation	0.06 mm	

4. Conclusions

In this paper, a stereo catadioptric system composed of two perspective digital cameras, a multimedia projector and a spherical mirror has been presented. The cameras have been assembled in a stereo-rig configuration and the mirror has been used to expand both cameras and projector field of view. Forward and Backward projection models have been developed and used to handle the catadioptric system calibration and the stereo-triangulation process. The calibration process has shown a Gaussian distribution of the re-projection error and a mean error value in the order of 0.15 pixels, thus validating the proposed forward projection model. The developed catadioptric system has been finally used to acquire the inner geometry of a target object characterized by a cylindrical region intersecting a conical region and a planar surface disposed at the bottom of the mirror. Results have highlighted an increase of the noise in the acquired data when the distance between the mirror and the target surface increases. The proposed optical setup is really compact, since it uses a single mirror. Moreover, it allows omnidirectional vision (360° field of view) allowing the reconstruction of target surfaces (also of internal geometries) with a single acquisition, without requiring multiple views and consequently any data registration process.

References

Agrawal, A., Y. Taguchi,S. Ramalingam (2010). Analytical Forward Projection for Axial Non-central Dioptric and Catadioptric Cameras. European Conference on Computer Vision, 6313, 129-143.

Almaraz-Cabral, C. C., J. J. Gonzalez-Barbosa, J. Villa, J. B. Hurtado-Ramos, F. J. Ornelas-Rodriguez,D. M. Cordova-Esparza, 2016. Fringe projection profilometry for panoramic 3D reconstruction. Optics and Lasers in Engineering 78, 106-112.

Barone, S., P. Neri, A. Paoli,A. Razionale, 2017. Optical Tactile Probe for the Inspection of Mechanical Components. Procedia Manufacturing 11(Supplement C), 1582-1591.

Barone, S., P. Neri, A. Paoli,A. V. Razionale, 2017. Forward and backward projection in catadioptric systems with spherical mirror: analytical solution and implementation. Submitted to Computer Vision and Image Understanding.

Barone, S., P. Neri, A. Paoli,A. V. Razionale (2017). Spherical mirror forward and backward projection. MATLAB Central, MathWorks.

Barone, S., A. Paoli,A. V. Razionale, 2017. Optical Tracking of a Tactile Probe for the Reverse Engineering of Industrial Impellers. Journal of Computing and Information Science in Engineering 17(4), 041003-041003-041014.

Bouguet, J. Y. (2015). Camera calibration toolbox for Matlab.

Boutteau, R., X. Savatier, J. Y. Ertaud,B. Mazari, 2008. An omnidirectional stereoscopic system for mobile robot navigation. 2008 International Workshop on Robotic and Sensors Environments, 138-143.
Fiala, M.,A. Basu, 2005. Panoramic stereo reconstruction using non-SVP optics. Computer Vision and Image Understanding 98(3), 363-397.
Goncalves, N.,H. Araujo, 2009. Estimating parameters of noncentral catadioptric systems using bundle adjustment. Computer Vision and Image Understanding 113, 11-28.
Hartig, F., H. Lin, K. Kniel,Z. Y. Shi, 2012. Standard conforming involute gear metrology using an articulated arm coordinate measuring system. Measurement Science & Technology 23(10).
Hartley, R. I.,P. Sturm, 1997. Triangulation. Computer Vision and Image Understanding 68(2), 146-157.
Jaramillo, C., R. G. Valenti,J. Z. Xiao, 2016. GUMS: A Generalized Unified Model for Stereo Omnidirectional Vision (Demonstrated via a Folded Catadioptric System). 2016 Ieee/Rsj International Conference on Intelligent Robots and Systems (Iros 2016), 2528-2533.
Kevin, H., 2013. Handbook of Optical Dimensional Metrology. Taylor & Francis.
Lin, S. S.,R. Bajcsy, 2003. High resolution catadioptric omni-directional stereo sensor for robot vision. 2003 Ieee International Conference on Robotics and Automation, Vols 1-3, Proceedings, 1694-1699.
Mian, S. H., M. A. Mannan,A. Al-Ahmari, 2015. Accuracy of a reverse-engineered mould using contact and non-contact measurement techniques. International Journal of Computer Integrated Manufacturing 28(5), 419-436.
Orghidan, R., J. Salvi,E. M. Mouaddib, 2003. Calibration of A Structured Light-Based Stereo Catadioptric Sensor, 2003 Conference on Computer Vision and Pattern Recognition Workshop.
Orghidan, R., J. Salvi,E. M. Mouaddib, 2006. Modelling and accuracy estimation of a new omnidirectional depth computation sensor. Pattern Recognition Letters 27(7), 843-853.
Perdigoto, L.,H. Araujo, 2013. Calibration of mirror position and extrinsic parameters in axial non-central catadioptric systems. Computer Vision and Image Understanding 117(8), 909-921.
Puig, L., J. Bermudez, P. Sturm,J. J. Guerrero, 2012. Calibration of omnidirectional cameras in practice: A comparison of methods. Computer Vision and Image Understanding 116(1), 120-137.
Ragot, N., J. Y. Ertaud, X. Savatier,B. Mazari, 2006. Calibration of a panoramic stereovision sensor : Analytical vs interpolation-based methods. Iecon 2006 - 32nd Annual Conference on Ieee Industrial Electronics, Vols 1-11, 4130-4135.
Rufli, M., D. Scaramuzza,R. Siegwart, 2008. Automatic Detection of Checkerboards on Blurred and Distorted Images, Proceedings of the IEEE/RSJ International Conference on Intelligent Robots and Systems (IROS 2008), Nice, France.
Scaramuzza, D., A. Martinelli,R. Siegwart, 2006. A toolbox for easily calibrating omnidirectional cameras. 2006 IEEE/RSJ International Conference on Intelligent Robots and Systems, Vols 1-12, 1-7.
Sturm, P., S. Ramalingam, J.-P. Tardif, S. Gasparini,J. Barreto, 2011. Camera Models and Fundamental Concepts Used in Geometric Computer Vision. Found. Trends. Comput. Graph. Vis. 6(1-2), 1-183.
Trujillo-Ortiz, A., R. Hernandez-Walls, K. Barba-Rojo,L. Cupul-Magana (2007). Roystest:Royston's Multivariate Normality Test. A MATLAB file.
Yoshizawa, T., 2015. Handbook of Optical Metrology: Principles and Applications, Second Edition. CRC Press.